Journal of Magnetics 13(3), 97-101 (2008)

Annealing Effect on Exchange Bias in NiFe/FeMn/CoFe Trilayer Thin Films

Ki-Yeon Kim[1]*, Hyeok-Cheol Choi[2], Chun-Yeol You[2], and Jeong-Soo Lee[1]

[1]*Neutron Science Division, Korea Atomic Energy Research Institute, Daejeon 305-353, Korea*
[2]*Department of Physics, Inha University, Incheon 402-751, Korea*

(Received 15 July 2008, Received in final form 26 August 2008, Accepted 28 August 2008)

We investigated the exchange bias fields at the NiFe/FeMn and FeMn/CoFe interfaces in 18.9-nm NiFe/15.0-nm FeMn/17.6-nm CoFe trilayer thin films as the annealing temperature was varied from room temperature to 250°C in a vacuum for 1 hour in a magnetic field of 150 Oe. Interestingly, magnetic hysteresis (M-H) measurements showed that NiFe/FeMn/CoFe trilayer thin films exhibited a completely contrasting variation of the exchange bias fields at both the NiFe/FeMn and FeMn/CoFe interfaces with annealing temperatures. High-angle X-ray diffraction (XRD) measurements indicated the absence of any discernible effect of thermal treatment on the NiFe(111) and FeMn(111) peaks. The compositional depth profile obtained from X-ray photoelectron spectroscopy (XPS) results presented the asymmetric compositional depth profiles of the Mn and Fe atoms throughout the FeMn layer. We contend that this asymmetric compositional depth profile and the preferential Mn diffusion into the NiFe layer, compared to that into the CoFe layer, are conclusive experimental evidence of the contrasting variation of the exchange bias fields at two interfaces having a common polycrystalline FeMn(111) layer.

Keywords : exchange bias, preferential Mn diffusion, XPS depth profile, thermal stability

1. Introduction

Due to the quantum confinement and proximity effects, the interface in magnetic thin film and multilayer structures exhibits unique magnetic properties, such as exchange bias phenomena between a ferromagnet (FM) and an antiferromagnet (AFM), and a spin dependent scattering between a FM layer and a nonmagnetic metal/oxide layer. These properties have found applications to novel spintronic devices such as giant magnetoresistance (GMR) spin valves and magnetic tunnel junctions (MTJs) in magnetic information technology [1].

The exchange bias is established after field cooling a magnetic heterostructure containing a FM/AFM interface across the AF blocking temperature or after depositing it in the presence of an *in situ* magnetic field [2]. The exchange coupling across a FM/AFM interface displaces the macroscopic magnetic hysteresis (M-H) loop of a FM layer along the field axis away from the origin and accompanies its enhanced coercivity. The amount of this displacement is called the exchange bias field. Although considerable progress has been made in the theory and experimental study during the last decade, a fundamental understanding of the exchange bias phenomena remains scientific challenging due to the inherently complex magnetic structure and the difficulty in directly probing a spin configuration and crystallographic structure at a FM/AFM interface [3].

One of the key technical problems in the feasible fabrication of GMR spin valves and MTJs is blocking the Mn diffusion into neighboring FM layers and enhancing their thermal stability. For example, after the preparation of exchange-biased FM/AFM(Mn family, metallic)/FM trilayer thin films having a common AFM such as NiFe/FeMn/NiFe and NiFe/IrMn/CoFe, thermal treatment is usually unavoidable and has an adverse effect on the thermal stability of the exchange bias field [4]. The migration of Mn atoms in an AFM layer into the neighboring oxide layers due to high oxygen affinity or interdiffusion across a FM/AFM interface during the annealing process are the predominant mechanisms of reducing the exchange bias field after thermal treatment [5, 6]. In this study, NiFe/FeMn/CoFe trilayer thin films were annealed in a vacuum for 1 hour in an applied field of 150 Oe as the annealing temperature was varied from

---

*Corresponding author: Tel: +82-42-868-4647
Fax: +82-42-868-4629, e-mail: kykim3060@kaeri.re.kr

120°C to 250°C. We have witnessed the contrasting variation of the exchange bias field at each interface. This can be ascribed to the asymmetric compositional depth profile of the Mn and Fe atoms and the preferential Mn diffusion into the NiFe layer, as compared to the CoFe layer from the X-ray photoelectron spectroscopy (XPS) sputter depth profile.

2. Experiment

Trilayers consisting of 18.9-nm NiFe(bottom)/15.0-nm FeMn/17.6-nm CoFe(top) were grown on Si(100)/SiO$_2$/5-nm Ta at an ambient temperature using dc magnetron sputtering at an Ar working pressure of 1.5 mTorr. A 5-nm Ta underlayer to promote a FeMn(111) texture and a 5-nm Ta capping layer to prevent oxidation were incorporated. The base pressure of the main chamber was below 2.0×10^{-9} Torr (UHV) and was attained within 2 hours of introducing the substrates into the main chamber from a fast entry. The NiFe, FeMn, and CoFe layers were consecutively deposited from Ni$_{80}$Fe$_{20}$, Fe$_{50}$Mn$_{50}$, Co$_{90}$Fe$_{10}$ alloy targets, respectively, with deposition rates of 0.472 Å/sec (Ta), 0.345 Å/sec (Fe$_{50}$Mn$_{50}$), 0.314 Å/sec (Ni$_{80}$Fe$_{20}$), and 0.498 Å/sec (Co$_{90}$Fe$_{10}$). Regarding the deposition geometry in the sputtering chamber, all of the magnetron sputtering guns were canted toward a sample holder rotating with a frequency of 30 rpm. A magnetic field of 300 Oe was applied along the sample plane during the deposition to induce the exchange anisotropy.

After growth of the films, they were annealed at temperatures ranging from 120°C to 300°C under a vacuum (10^{-7} Torr) for 1 hour in an applied field of 150 Oe. Crystallographic structures such as the film thickness, surface/interface roughness and growth texture were characterized by low-angle X-ray reflectivity (XRR) and high-angle $\theta/2\theta$ X-ray diffraction (XRD). High-angle XRD confirmed the highly (111) oriented texture of the FeMn and NiFe layers, as shown in Fig. 1(a). Each layer and its roughness, as calculated from the XRR in Fig. 1(b), are summarized in Table 1. M-H loops were measured by a vibrating sample magnetometer (VSM) and the compositional depth profiles by XPS.

XPS sputter depth profiles were obtained by using a K-Alpha XPS instrument (Thermo Fisher Scientific Ltd). A sample surface of dimensions 1 mm×0.5 mm was erased with an etch rate of about 43 Å/min by a 1 keV Ar ion beam, while a central part of dimensions 200 μm × 200 μm inside the etched surface was irradiated with a monochromatic X-ray beam generated from Al Kα (1486.6 eV), which caused the photoelectrons to be emitted with a take-off angle of 90 degree from the sample surface. If λ is the inelastic mean free path of the emerging electron, the vertically detectable sampling depth d is given by d=3 λ [7]. Experimental d values for several elements were determined to be 2.3 nm in a literature review by Tamuma *et al.* [8]. XPS depth profiles of all the elements in the Si(100)/SiO$_2$/Ta/NiFe/FeMn/CoFe/Ta thin films were recorded by an electron energy analyzer with a pass energy of 1.0 eV.

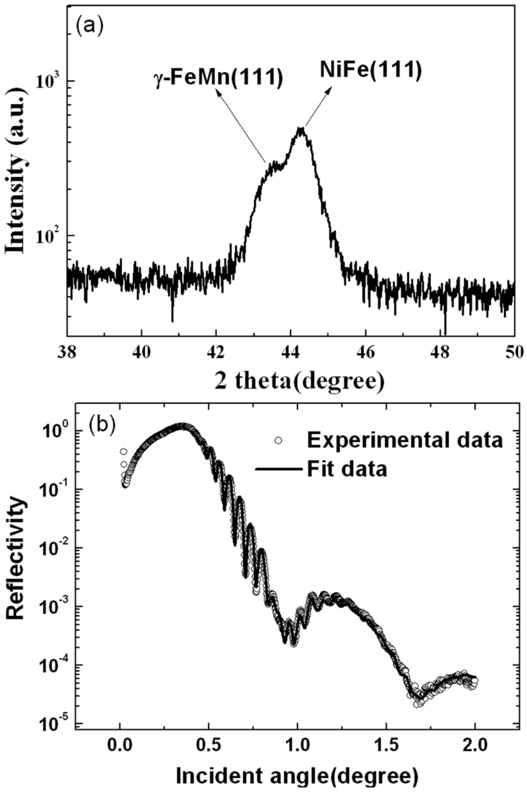

Fig. 1. (a) High-angle $\theta/2\theta$ x-ray diffraction of the NiFe/FeMn/CoFe trilayer thin films with a 5-nm Ta underlayer (b) Low-angle x-ray reflectivity as a function of an incident angle of the NiFe/FeMn/CoFe trilayer thin film where each layer thickness and its roughness are calculated from fit to the experimental data.

3. Results and Discussion

Fig. 2 shows the representative M-H loops of the NiFe/FeMn/CoFe trilayer thin film measured at room temperature (RT) and 150°C along both the in-plane direction, which is the same as the magnetic field applied during the sample preparation, and perpendicular to the film plane. The in-plane M-H loop in Fig. 2(a) shows a square-like and biased hysteresis shape with well-defined switching fields where the NiFe and CoFe layers are shifted by −84 Oe and −6 Oe at RT, respectively. On the other hand, the perpendicular one in Fig. 2(b) shows a slanted and

Table 1. Thickness and roughness of each layer calculated from fit to low-angle x-ray reflectivity of the NiFe/FeMn/CoFe trilayer thin films.

	Si/SiO_2	Ta	NiFe	FeMn	CoFe	Ta	Ta_2O_5
Thickness (nm)	500000	5.49	18.87	15.03	17.57	4.73	2.25
Roughness (nm)	0.45	0.52	1.1	0.8	1.59	1.47	1.25

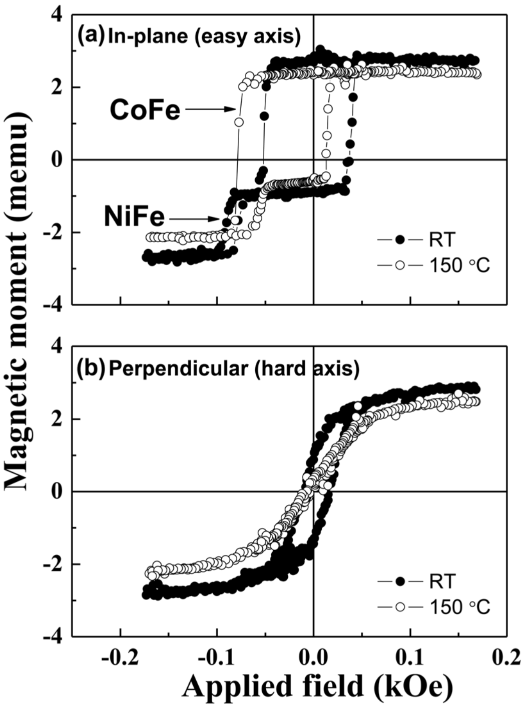

Fig. 2. (a) In-plane and (b) perpendicular M-H loops of the NiFe/FeMn/CoFe trilayer thin films at RT and 150 °C. In-plane M-H loop shows a square and exchange-biased hysteresis shape, while perpendicular one shows a slanted and unbiased hysteresis shape.

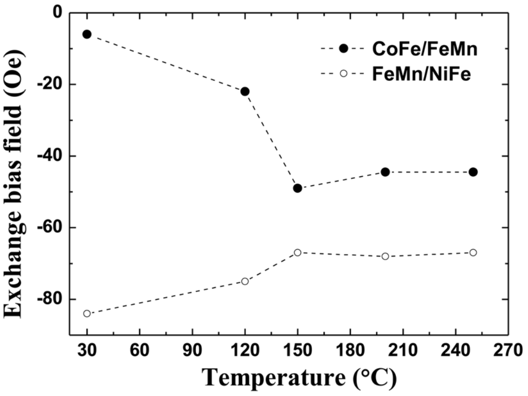

Fig. 3. Exchange bias field as a function of the annealing temperatures from RT to 250°C in the NiFe/FeMn/CoFe trilayer thin films which are annealed for 1 hour in a vacuum with a magnetic field of 150 Oe. Empty (filled) circles represent the NiFe/FeMn(FeMn/CoFe) interfaces.

unbiased shape. Saturation magnetizations from the M-H loops of the NiFe and CoFe layers were 381.5 emu/cm^3 and 853.8 emu/cm^3, and were about half the size of the corresponding bulk values [9]. This discrepancy indicated the existence of magnetic dead layers at the Ta/NiFe and CoFe/Ta interfaces or the decrease in the Curie temperature of the FM layer with decreasing layer thickness due to the proximity effect [10, 11]. However, further discussion on this issue is beyond the scope of this paper.

After thermal treatment at different temperatures ranging from 120°C to 250°C for 1 hour in a magnetic field of 150 Oe, the exchange bias field in the NiFe/FeMn interface was decreased from −84 Oe at RT to −67 Oe at 250 °C, while that in the FeMn/CoFe interface was increased from −6 Oe at RT to −44.5 Oe at 250°C, as shown in Fig. 3. To understand the annealing temperature dependence of the exchange bias field in our system, we conducted XRD measurement of the NiFe(111) and γ-FeMn(111) textures at different annealing temperatures, as presented in Fig. 4. The XRD results indicated the absence of any distinguishable structural change of the NiFe and FeMn layers at annealing treatment temperatures up to 250°C in the NiFe/FeMn/CoFe trilayer thin films. This demonstrated that the texture was not the main factor in the variation of the exchange bias field with annealing temperature in our systems.

To further clarify the annealing effect on the exchange

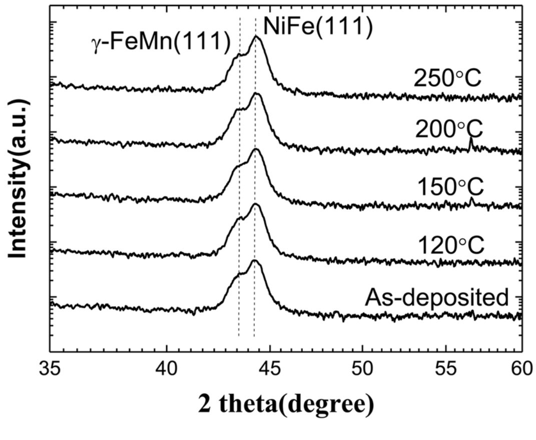

Fig. 4. High-angle $\theta/2\theta$ x-ray diffraction peaks of NiFe(111) and γ-FeMn(111) phases at different annealing temperatures from RT to 250°C.

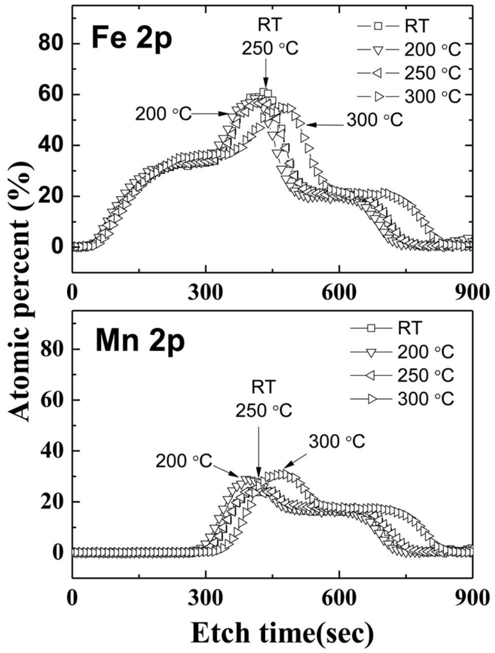

Fig. 5. XPS sputter depth profiles of Fe 2p and Mn 2p in the NiFe/FeMn/CoFe trilayer thin films at different annealing temperatures from RT to 300°C.

bias field in our system, we conducted XPS depth profile measurement with a 1 keV Ar ion beam with an etch rate of about 43 Å/min. Fig. 5 shows the XPS sputter depth profiles of the Fe 2p and Mn 2p as the annealing temperature was varied from RT to 300°C. Although the NiFe/FeMn and FeMn/CoFe interfaces could not be defined correctly in the depth profile data, the peak positions of Mn 2p and Fe 2p inside the FeMn layer were definitely asymmetric at all annealing temperatures, indicating that the alloy composition was not uniform throughout the FeMn layer and that the Mn composition near the CoFe/FeMn interface was higher than that near the FeMn/NiFe interface. Parkin *et al*. reported a concentration gradient across an FeMn layer in as-grown Si(111)/40-nm NiFe/40-nm FeMn/30-nm Ta thin films from an Auger sputter depth profile with approximately $Fe_{50}Mn_{50}$ at the FeMn/Ta interface and $Fe_{45}Mn_{55}$ at the NiFe/FeMn interface [12].

If the sputtering rates of the Fe and Mn atoms are similar to each other and there is no preferential diffusion during an etching by an Ar ion beam, the XPS sputter depth profiles provide valuable information indicating that the depth profiles of the Fe and Mn atoms must be not homogeneous in the FeMn layer. However, the reason that the gradient FeMn compositions are completely opposite between the results of Parkin's study and our own remains unanswered. Furthermore, the XPS sputter depth profiles clearly demonstrate that after annealing at 300°C, the Mn and Fe atoms in the FeMn layer preferentially diffuse into the NiFe layer, rather than into the CoFe layer, because the Mn and Fe atoms can easily diffuse into a NiFe layer with its lower density than that of a CoFe layer [13]. Therefore, both the diffused and as-deposited interfaces are better defined and closer to the $Fe_{50}Mn_{50}$ composition for the FeMn/CoFe interface, compared to the NiFe/FeMn interface. It is well-known that $Fe_{50}Mn_{50}$ is a prerequisite to maximize the exchange bias field in FM/FeMn systems. We contend that the asymmetric compositional depth profiles of the Mn and Fe atoms throughout the FeMn layer and the preferential Mn diffusion into the NiFe layer are conclusive evidence of the annealing temperature dependence of the exchange bias fields in the NiFe/FeMn/CoFe trilayer thin films with a Ta underlayer and a Ta capping layer.

4. Conclusion

Exchange-biased NiFe/FeMn/CoFe trilayer thin films with a Ta underlayer and a Ta capping layer were fabricated using a magnetron sputtering technique. Exchange bias fields were calculated from the M-H loops measured by VSM and exhibited a contrasting variation between the NiFe/FeMn and FeMn/CoFe interface layers as the annealing temperature was varied from RT to 250°C. No distinguishable structural change was evident in the XRD measurements, indicating that the texture was not the main factor in the variation of the exchange bias field with annealing temperature in our systems. The XPS sputter depth profiles revealed that the depth profiles of the Fe and Mn atoms in the FeMn layer were not homogeneous and that the Mn atoms in the FeMn layer were diffused preferentially into the NiFe layer, rather than the CoFe layer. We regard this as conclusive evidence of an annealing temperature dependence of the exchange bias field in our systems.

Acknowledgment

This work was supported by KOSEF (Nuclear R&D program, Basic Research Program (No. R01-2007-000-20281-0)) through a grant provided by the Korea government (MEST).

References

[1] Pratap Kollu, Doung Young Kim, and Cheol Ki Kim, J. Magnetics **13**, 1 (2008).
[2] M. Tsunoda and M. Takahashi, J. Magnetics **7**, 80 (2002).
[3] F. Radu and H. Zabel, Exchange Bias Effect of Ferro-/

Antiferromagnetic Hetero structures, STMP **227**, 97 (2007).

[4] J. H. Lee, H. D. Jeong, C. S. Yoon, C. K. Kim, B. G. Park, and T. D. Lee, J. Appl. Phys. **91**, 1431 (2002).

[5] S. W. Kim, J. K. Kim, J. H. Kim, B. K. Kim, J. Y. Lee, S. S. Lee, D. G. Hwang, and J. R. Rhee, J. Appl. Phys. **93**, 6602 (2003).

[6] C. S. Yoon, J. H. Lee, and C. K. Kim, J. Appl. Phys. **93**, 8910 (2003).

[7] D. Briggs and M. P. Seah, Practical Surface Analysis by Auger and X-ray Photoelectron Spectroscopy, John Wiley & Sons Ltd, Chichster (1983) p. 133.

[8] S. Tanuma, C. J. Powell, and D. R. Penn, Surf. Anal. **11**, 577 (1998).

[9] R. C. O'Handley, Modern Magnetic Materials: Principles and Applications, John Wiley & Sons, Inc., New York (2000). p. 99.

[10] M. Kowalewski, W. H. Butler, N. Moghadam, G. M. Stocks, T. C. Schulthess, K. J. Song, J. R. Thompson, A. S. Arrott, T. Zhu, J. Drewes, and R. R. Katti, J. Appl. Phys. **87**, 5732 (2000).

[11] R. Zhang and Roy F. Willis, Phys. Rev. Lett. **86**, 2665 (2001).

[12] S. S. P. Parkin, V. R. Deline, R. O. Hilleke, and G. P. Felcher, Phys. Rev. B **42**, 10583 (1990).

[13] Young Deung Kim, Kap Soo Yoon, Ja Hyun Koo, Ki Woong Kim, Chae Ok Kim, and Jin Pyo Kim, J. Korean Phys. Soc. **45**, 683 (2004).